BARRIER EFFECT IN CO_2 CAPTURE AND STORAGE FEASIBILITY STUDY

[1)]G. Montegrossi, [2)] B. Cantucci, [3)]G. Bicocchi, [1,3)]O. Vaselli, [2)]F. Quattrocchi

1) CNR – IGG, Via G. La Pira 4, 50121 Florence, Italy
2) INGV, Via Vigna Murata 605, 00141 Roma, Italy
3) University of Florence, Dept. Earth Sciences, Via G. La Pira 4, 50121 Florence, Italy
e-mail: montegrossi@igg.cnr.it

ABSTRACT

CO_2 Capture & Storage (CCS) in saline aquifer is one of the most promising technologies for reducing anthropogenic emission of CO_2. Feasibility studies for CO_2 geo-sequestration in Italy have increased in the last few years. Before planning a CCS plant an appropriate precision and accuracy in the prediction of the reservoir evolution during injection, in terms of both geochemical calculation and fluid flow properties, is demanded. In this work a geochemical model will be presented for an offshore well in the Tyrrhenian Sea where the injection of 1.5 million ton/ year of CO_2 is planned. The dimension of the trapping structure requires to study an area of about 100 km^2 and 4 km deep. Consequently, three different simulations were performed by means of TOUGHREACT code with Equation Of State module ECO2N.
The first simulation is a stratigraphic column with a size of 110*110*4,000 meters and a metric resolution in the injection/cap-rock area (total of 8,470 elements), performed in order to asses the geochemical evolution of the cap-rock and to ensure the sealing of the system. The second simulation is at large scale in order to assess the CO_2 path from the injection towards the spill point (total of about 154,000 elements).
During this simulation, the effect of the full coupling of chemistry with fluid flow and a relevant effect in the expected CO_2 diffusion velocity was recognized. Owing to the effect of chemical reaction and coupling terms (porosity/permeability variation with mineral dissolution/precipitation), the diffusion velocity results to be 20% slower than in a pure fluid flow simulation. In order to give a better picture of this 'barrier' effect, where the diffusion of the CO_2-rich acidic water into the carbonate reservoir originates a complex precipitation/dissolution area, a small volume simulation with a 0.1 m grid was elapsed. This effect may potentially i) have a big impact on CO_2 sequestration due to the reduction of available storage volume reached by the CO_2 plume in 20 years and/or the enhanced injection pressure and ii) outline the relevance of a full geochemical simulation in an accurate prediction of the reservoir properties.

DATA ACQUISITION

The petrophysical data used in the simulations of CO_2 injection described in the present work were obtained in a previous study (Montegrossi et al. 2008). A brief report of the procedure is here reported. Each formation recognized from the well-log (Table 1), was collected in-shore.

Table 1. Average pressure (P) and temperature (T) for each formation are reported. K_i: permeability, φ_i: initial porosity, φ_c: critical porosity.

Formation	Zone	P bar	T °C	Density kg/m^3	Cond. T. W/m °C	Capac. T. J/kg 25°C	K_i m^2	φ_i	φ_c
Gray Clay	1	24	25	2400	02.08.00	1280	2.95e-17	0.14	-
Carbonatic Flysch	2	46	32	2600	2.21	940	7.65e-18	0.03	-
Sandstone	3	115	55	2500	2.55	1370	7.65e-18	0.03	-
Clay Shale	4	181	76	2600	1.70	1170	7.65e-18	0.03	-
Schist	5	189	79	2600	1.70	870	2.04e-17	0.05	-
Limestone and Jasperoids	6	193	80	2600	2.13	900	2.04e-17	0.05	0.046
Cherty Limestones	7	204	84	2600	2.13	920	2.04e-17	0.10	0.055
Marly Limestones	8	213	87	2600	2.04	940	1.02e-16	0.10	0.044
Limestones	9	232	93	2600	2.04	940	2.48e-14	0.10	0.055
Dolomite Limestones	10	280	108	2600	1.96	940	2.48e-14	0.10	0.055
Anhydrites	11	308	118	2800	4.08	1870	1.84e-16	0.06	0.043

The mineralogical composition was calculated by combining calcimetric determination with a Dietrich-Fruhling apparatus for calcite and a XRD Rietveld analysis to quantify the main minerals. A correction for dolomite was applied to the calcimetry determination. Rietveld quantification procedure was performed by using Maud v2.2. After the separation of the clay fraction (<2 μm), clay minerals were determined by XRD with the analysis of oriented-, glycol- and 450 and 600 °C treated samples. The key concept of the models is that, once defined the mineralogy of each geological formation, a relationship among thermal capacity, conductivity, porosity and permeability can be established (Montegrossi et al. 2008). The thermal properties are computed by simply using a weighted sum of the thermal properties of each mineral, using 1% porosity as initial value by literature data (Singh et al. 2007, Clauser & Huegens 1995). Being the well offshore, we can indeed reasonably assume that the rock pores are filled with water, and they obviously have thermal properties sensibly different from those of minerals: the higher the porosity, the lower the thermal capacity and conductivity. The limit of this model is the assumption that no turbolent heat transport is present. This is true for up to 10^{-12} m/s values of permeability. Thus, the thermal properties are expressed as a function of porosity.

Correlation model between porosity and permeability are well known and they are function of the main mineralogical composition of each stratum. On the basis of the mineralogical analysis reported in Table 2, we decided to use a clay coating for the upper formations (Zone 1-5, Table 1) and a calcite coating for the other strata (Zone 6-11, Table 1).

Table 2. Mineralogical composition (volume fraction) of considered formations in the model.

Zone	Calcite	Quartz	Dis. Dolom.	K-felds.	Smectite	Illite	Chlorite	Kaolinite	Muscov..	Montmor.	Anhyidr..	Dawsonite	Calcedony	Phlogopite
1	0.2559	0.0698	0.0155	0.062	0.185	0.0035	0.0606	0.025	0.0785	1e-05	-	1e-05	1e-05	1e-05
2	0.9520	0.0307	1e-05	-	-	0.0130	0.0012	1e-05	-	0.0028	-	1e-05	1e-05	1e-05
3	0.7041	0.1558	0.0176	-	-	0.0513	0.0202	1e-05	-	0.0404	-	1e-05	1e-05	1e-05
4	0.8380	0.0536	1e-05	-	-	0.0350	0.0324	1e-05	-	0.0410	-	1e-05	1e-05	1e-05

5	0.6105	0.3595	1e-05	-	-	0.0118	0.0021	1e-05	-	0.0152	-	1e-05	1e-05	1e-05
6	0.9540	0.0336	1e-05	-	-	0.0123	-	1e-05	-	1e-05	-	1e-05	1e-05	1e-05
7	0.6630	0.3140	1e-05	-	-	0.0020	0.0015	1e-05	-	0.0196	-	1e-05	1e-05	1e-05
8	0.9610	0.0367	1e-05	-	-	-	-	1e-05	-	0.0020	-	1e-05	1e-05	1e-05
9	0.9941	0.0059	1e-05	-	-	-	-	1e-05	-	1e-05	-	1e-05	1e-05	1e-05
10	0.7478	0.0060	0.2398	-	-	-	-	1e-05	-	0.0064	-	1e-05	1e-05	1e-05
11	0.0080	-	0.0020	-	-	-	-	-	-	-	0.989	1e-05	1e-05	-

A coating model assumes the presence of small channel whose tortuosity and connectivity depend on the filling material, that is calcite or clay in our assumption, with a correction for the presence of quartz as vein filler material. A summary of the correlation models is reported in Table 1, using the equations of Verma and Pruess (1988) and Steefel and Lasaga (1994) for Zone 6-11 (with n = 5) and Zone 1-5, respectively.

Once a correlation model between porosity and permeability is established, the porosity is the only independent variable in our system. For the calculation we used the software package SHEMAT (Kuhn and Chiang, 2003) that also allows to compute the heat flow due to fluid advection. As boundary condition the surficial heat flow reported in Calore et al. (1988) was considered.

With a try-and-error procedure the best fit between our temperature profile and the well-log temperature profile was computed, thus obtaining a porosity profile. From the model, detailed temperature, porosity and permeability profiles and the thermal properties for each rock formation were calculated (Table 1).

In order to construct a geochemical model, the database of Wolery (1992) was adopted. The database is to be corrected to take into account the pressure: the pressure of the centroid of the reservoir unit (namely Cherty Limestone Formation), which is 204 bar, was used. The pressure correction of the database was performed by means of SUPCRT92 (Johnson et al., 1992).

The pristine formation water was computed by means of PHREEQC 2.15 (Parkhurst and Appelo, 1999) using the NaCl-equivalent salinity measured in the well log, as suggested by Cantucci et al. (2009), with the pressure corrected database.

The same database was also used for the TOUGHREACT (Xu and Pruess, 2001; Xu et al., 2006) model with the specific Equation Of State for CO_2 (ECO2N EOS, Spycher and Pruess, 2005).

The geochemical model strategy proceeds through a fully kinetic approach. The kinetic database is from Palandri and Kharaka (2004 and references therein), the acquisition of the mineral specific surface was performed with a geometric approach based on a morphology investigation carried out by means of a Scanning Electron Microscope equipped with an Energy Dispersive System (SEM-EDS), that measures for each mineral the isodistribution of the grain size, which is then transformed into a specific reaction area (Table 3) and converted according to the geometric grain shape used in TOUGHREACT. For secondary minerals, an area corresponding to a 10^{-6} m radius grain size was adopted.

The relative permeability and capillary pressure equation used are from Corey (1954), with an irreducible liquid saturation assumed at 0.1.

The diffusivity coefficients of water and CO_2 were computed according to Palmer (1994), Frank et al. (1996), Wang et al. (1996), Hashimoto and Suzuki (2002), Tamini et al. (1994) from viscosity of the fluids at the reservoir temperature and the resulting diffusion coefficients are 4.04 10^{-9} m^2/s for water and 1.59 10^{-3} m^2/s for CO_2.

Table 3. Minerals reactive surface (Area) computed as geometric area from SEM-EDS morphological analysis. Bold: Reactive surface of secondary minerals with initial radium of $1x10^{-6}$ m.

Zona	1	2	3	4	5	6	7	8	9	10	11
	Area cm^2/g	Area Cm^2/g	Area cm^2/g	Area cm^2/g	Area cm^2/g	Area cm^2/g	Area cm^2/g	Area cm^2/g	Area cm^2/g	Area cm^2/g	Area cm^2/g
Calcite	5844.4	2859.2	71.480	2144.4	4108.2	3160.0	10236	4435.6	4435.6	6653.4	634.55
Dolomite	68.208	**3769.2**	**3769.2**	**3769.2**	**3769.2**	**3769.2**	**3769.2**	**3769.2**	**3769.2**	9767.5	605.50

Quartz	5976.7	10544	349.61	1271.5	6845.7	751.75	680.41	336.86	336.86	618.55	-
K-feld.	6211.1	-	-	-	-	-	-	-	-	-	-
Smectite	6599.3	-	-	-	-	-	-	-	-	-	-
Illite	5759.4	6363.6	1636.4	3636.4	1621.9	7785.2	6556.7	-	-	-	-
Chlorite	5596.6	6183.7	1374.2	3553.6	1576.1	-	6371.3	-	-	-	-
Montmor.	**5325.7**	8706.5	1954.5	4975.1	2219.0	**5325.7**	8970.6	-	-	11608	-
Anhydride	-	-	-	-	-	-	-	-	-	-	933.37
Muscov.	5596.6	-	-	-	-	-	-	-	-	-	-
Kaolinite	6045.1	**4085.7**	**4085.7**	**4085.7**	**4085.7**	**4085.7**	**4085.7**	**4085.7**	**4085.7**	**4085.7**	**4085.7**
Dawsonite	**4351.5**	**4351.5**	**4351.5**	**4351.5**	**4351.5**	**4351.5**	**4351.5**	**4351.5**	**4351.5**	**4351.5**	**4351.5**
Calcedony	**4039.5**	**4039.5**	**4039.5**	**4039.5**	**4039.5**	**4039.5**	**4039.5**	**4039.5**	**4039.5**	**4039.5**	**4039.5**
Phlogopite	**3782.5**	**3782.5**	**3782.5**	**3782.5**	**3782.5**	**3782.5**	**3782.5**	**3782.5**	**3782.5**	**3782.5**	**-**

MODELLING STRATEGY

The data show that the reservoir, located in the Cherty Limestone Formation, show low permeability value and medium porosity value. The limiting factor of CO_2 injection in such a system is either the velocity of the displaced water or the injection overpressure needed to provide the expected injection rate; the request is an injection rate of 1.5 Mton/year for 20 years. A first study on the whole structure without chemistry, by considering only CO_2 solubility, leads to the conclusion that the injection overpressure should be 40 bars to obtain the desired injection rate. The same overpressure leads to a lower injection rate while using a fully coupled model, with a kinetic model for mineral reactions and a variable porosity-permeability model with the correlation curves reported in Table 1.

In order to study which changes could induce such variations, an horizontal model from aside of the CO_2 plume to a point of water displacement was realized, then a column model, and the results were used to plan an injection strategy for the whole structure model.

HORIZONTAL PATHWAYS

The horizontal model is made by 99x11x11 elements, each one being a cube with 1 m long side. The reservoir conditions were considered, i.e. 200 bars of pressure and a left side CO_2 plume with 40 bars of overpressure, located in the central element of the left hand side of the model. On the bottom of the right side there is a 'spill point', simulated as an extraction well for water on deliverability at 201 bars. The results are summarized in Figure 1, where the contour lines are reported for a permeability of 10^{-20} m^2 after 2 years of simulation. On the left-hand side, near the CO_2 plume, there is a small increase in permeability (original permeability was 2,040 10^{-20} m^2), and on top of the model an area of slightly increased permeability is observed. This is due to the buoyancy of the $CO_{2(aq)}$-rich water with respect to normal water, then the water goes through the spill point on the right-hand bottom side of the figure; since the $CO_{2(aq)}$ rich water shows a pH of 6,6 is slightly aggressive with respect to the calcite in the Cherty Limestone Formation, thus along the migration pattern a slight increase in the permeability is observed. The upper pattern will be filled by $CO_{2(g)}$. The red-colored area, mainly on the bottom of Figure 1, where permeability decrease to 2,038 10^{-20} m^2, denotes the deposition of secondary calcite. In order to study this effect, a simulation of the stratigraphic column was performed.

Figure 1 Simulation of the horizontal well after 2 years of simulation time. Numbers represent permeability in 10^{-20} m^2, colors represent porosity change from -0.002 (blue), 0.0 (green), to +0.002 (red)

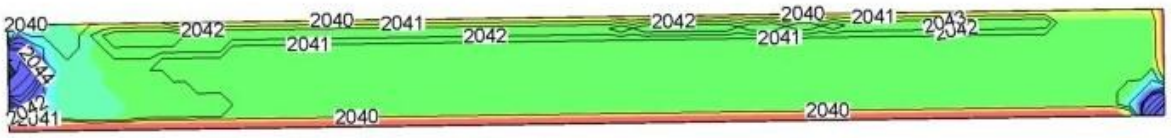

THE COLUMN MODEL

The column model is made of 10 m long 11x11 elements on X- and Y-axis, and 70 elements on Z-axis, whose dimensions are 10 m in the Zone from 5 to 8 (Table 1). The injection is performed at the center of the reservoir zone, i.e. at a depth of 1900 m and a pressure of 190 bars (hydrostatic pessure) plus 40 bars of injection overpressure. The spill point is at a depth of 2400 m on deliverability at hydrostatic pressure. After five years of simulations, an increased permeability area around the injection point and a lowered permeability area below the injection point are highlighted. From the permeability contour we could define a convective cell generated by the buoyancy of the $CO_{2(aq)}$-rich water and the more dense water originated by calcite dissolution. The nearly saturated water at acidic pH migrates downward, and when it encounters the reservoir basic water $CO_{2(aq)}$ is neutralized. The pH increase gives rise to a deposition of secondary calcite and, at a minor extent (0.01%), dolomite. Carbonates are in fact the only minerals in the simulation able to form deposits outside the CO_2 plume, being the other secondary minerals depositing only within the plume. Nevertheless, the carbonate dissolution effect on porosity and permeability is by far the most important process, also due to theyr generally faster kinetic. Summarizing, around the injection point the permeability increases up to 2,075 10^{-20} m^2 and a barrier is formed downward due to water stratification (Figure 2). This effect is apparently small, but it is important to outline that it is due mainly to the dissolved calcite, that will precipitate when the acidic saline water are diluted in the reservoir water.

Figure 2 Column after 5 years of simulation. Numbers represent permeability in 10^{-20} m^2, on the left-hand side the 3D image of 2,040 10^{-20} m^2 contour is reported, while on the right-hand side the 2D vertical corresponding section is drawn; elements are 10x10x10 m.

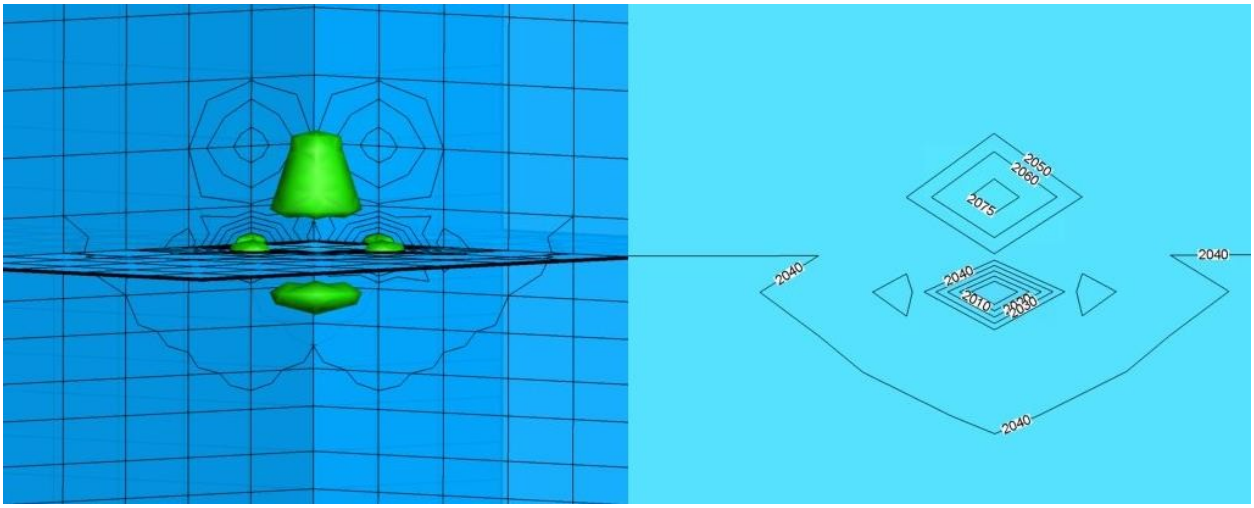

STRUCTURE MODEL

The grid of the trapping structure is made by 54x51x55 (151,470) elements, with dimensions of 250x250 m along the X- and Y-axis, and variable Z with a thickness of 10 m in the reservoir units (Zone 5-8) (dark green, Figure 3). The irregular hexahedric elements follow the contact surfaces between the different geological formations, being the structure obtained directly by seismic data. This kind of structure, though very common in nature for shape and dimension, requires long computation times with a relatively low resolution. On the basis of the previous simulation, the position of the injection point was located on the middle of the reservoir along the Z-axis, and shifted on the right boundary of the cap-rock (Fig. 3, pink dot). This is due to the fact that the $CO_{2(aq)}$-rich water and $CO_{2(g)}$ originated around the injection point will arise up to the top of the structure along the cap-rock boundary. The Ca^{2+}-HCO_3^- enriched solution will move down along the side of the structure, thus protecting the cap-rock and allowing to fill out of CO_2 the right side of the structure, that may not be available for CO_2 storage, otherwise. As the injection was performed, the injection pressure was adjusted to obtain 1.5 MTon CO_2/year. The result was an injection pressure of 190 bars of hydrostatic pressure and 50 bars of injection overpressure. A simulation on both the CO_2 flux and mineral precipitation leads to the results shown in Figure 4. After 5 years of simulation, there is a contribution to SMCO2 (Total CO_2 sequestered in mineral phases) almost only related to calcite, that reaches its maximum just out of the spill point, all around the structure with an average value of about 0.02 Kg/m^3. Just at the outlet of the structure the elements show a slightly increased permeability (2,360 10^{-20} m^2 with respect to the reference value of 2,040 10^{-20} m^2), while the main depositing elements are just the nearest elements outside the structure (250 m away) and show a permeability of 260 10^{-20} m^2. The escaping pathways of the displaced water, lined along Y-axis in Figure 4, show a permeability value of 1,240 10^{-20} m^2, thus being the main permeability barrier very localized. Along the Z-axis the flux is limited by the marly limestone formation, were, due to the interaction with basic reservoir water, the formation of a depositing area just along the contact of the two strata beds is favoured and show the same permeability barrier effect observed on the spill point level.

Figure 3 Structure meshing – 54x51x55 elements, with dimensions of 250x250 m along X- and Y-axis, and variable Z with 10 m thick elements in the reservoir (dark green). Pink dot is the injection point.

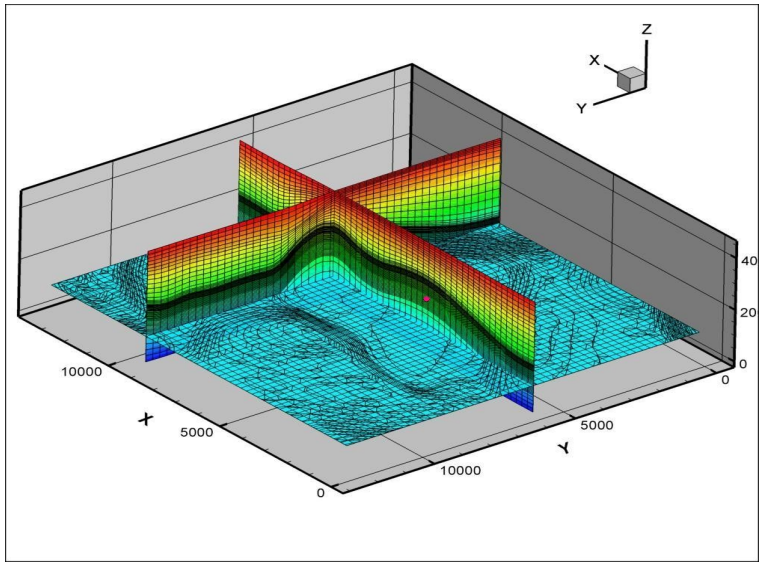

Figure 4 SMCO2, Total sequestered CO_2 in mineral phases in kg m^{-3} medium, the blue dot shows the position of the spill point, and all around the structure the precipitating area at the spill point level.

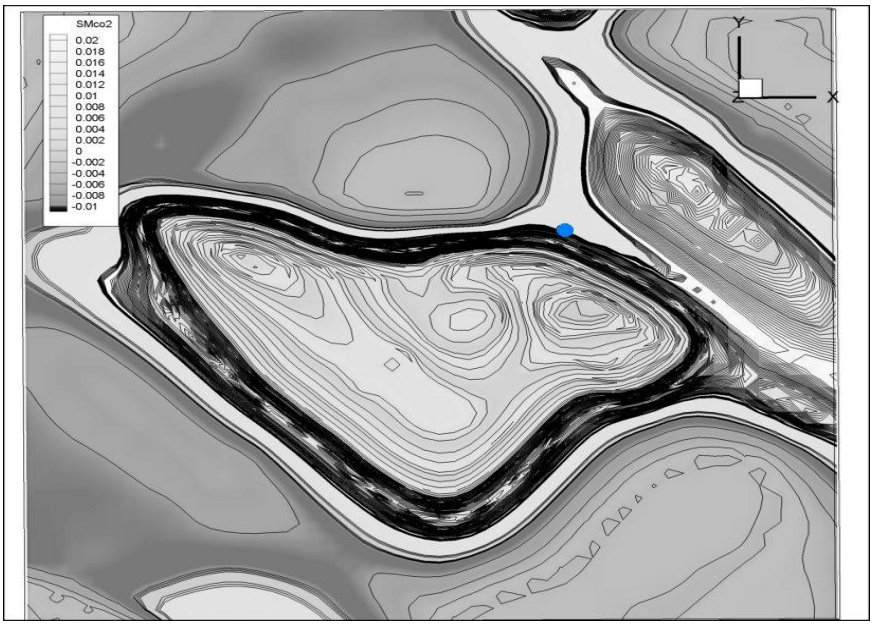

CONCLUSION

Permeability plays an important role in CO_2 injection, especially in a low permeability reservoir. In this work we show that an important effect, mainly due to the formation of secondary calcite deposits on the spill point, occurs. The depositing site is where the water displaced from the trapping structure encounters the 'fresh' water of the reservoir. This process is relatively fast, and the secondary calcite barrier is fully formed just after 5 years of injection in a large (5x3x0.5 km) trapping structure; the barrier reduces the outflow velocity of the CO_2–displaced water, thus reflecting in a lower CO_2 injectivity. Low permeability reservoir may present many difficulties, but the low permeability itself guarantees against CO_2 leakage, therefore a major effort should be done in order to study this kind of systems.

REFERENCES

Calore C., R. Celati, P. Squarci, L. Taffi, *Temperature map of Italy at 1000, 2000 and 3000 m*, Intl. Inst. for Geothermal Research-CNR, Pisa, 1988.

Cantucci, B., G. Montegrossi, O. Vaselli, F. Tassi, F. Quattrocchi, and E.H. Perkins, *Geochemical modeling of CO_2 storage in deep reservoirs: The Weyburn Project (Canada) case study*, Chemical Geology, 265, Issues 1-2, 181-197, 2009

Clauser C. & Huenges E., *Thermal Conductivity of Rocks and Minerals, Chapter 3 of A Handbook of Physical Constants.* AGU Ref. Shelf 3, 1995

Corey, A.T. *The Interrelation Between Gas and Oil Relative Permeabilities*, Producers Monthly, 38-41, November 1954.

Frank M.J.W., Kuipers J.A.M., Van Swaaij W.P.M., *Diffusion Coefficients and viscosities of CO_2+H_2O, CO_2+CH_3OH, NH_3+H_2O, and NH_3+CH_3OH Liquid Mixtures*, J. Chem. Eng. Data, 41, 297-302, 1996.

Hashimoto S. and Suzuki M., *Vertical distribution of carbon dioxide diffusion coefficients and production rates in forest soils*, Soil. Sci.Soc.Am.J., 66, 1151-1158, 2002.

Kuhn M., and W.-H. Chiang, *Processing Shemat, Ver. 4.0.0, SHEMAT Ver. 8.0*, J. Bartels, C. Clauser, M. Kuhn, D. Mottaghy, V. Rath, R. Wagner & A. Wolf, Springer-Verlag, Berlin, Heidelberg, 2003.

Johnson, J.W., E.H. Oelkers, H.C. Helgeson, *SUPCRT 92: A software package for calculating the standard molal thermodynamic properties of minerals, gases, aqueous species, and reactions from 1 to 5000 bars and 0 to 1000 °C*. Comput. Geosci. 18, 899-947, 1992..

Lutterotti, L., S. Matthies, H-R. Wenk, *MAUD (Material Analysis Using Diffraction): a user friendly*

Java program for Rietveld Texture Analysis and more, Proceeding of the Twelfth International Conference on Textures of Materials (ICOTOM-12), 1, 159, 1999.

Montegrossi, G., B. Cantucci, O. Vaselli, and F. Quattrocchi, *Reconstruction of porosity profile in an off-shore well,* Bollettino di Geofisica Teorica ed Applicata, 49 (2), 408-410, 2008.

Palandri, J., Y.K. Kharaka, *A compilation of rate parameters of water–mineral interaction kinetics for application to geochemical modelling*, US Geol Surv. Open File Report 2004-1068, 2004, p. 64.

Palmer, B.J, Calculation of thermal-diffusion coefficients from plane-wave fluctuations in the heat energy density, Physical Review E, 49 (3), 2049-2057, 1994.

Parkhurst, D.L., C.A.J. Appelo, *User's guide to PHREEQC (version 2)-A computer program for speciation, batch-reaction, one-dimensional transport, and inverse geochemical calculations*, U.S. Geological Survey Water-Resources Investigations Report 99-4259, pp. 312, 1999.

Singh T.N., Sinha S., Singh V.K., *Prediction of thermal conductivity of rock through physico-mechanical properties.* Building and Environment, 42, 146–155, 2007

Spycher, N., K. Pruess, *CO_2–H_2O mixtures in the geological sequestration of CO_2 center dot. II. Partitioning in chloride brines at 12–100 °C and up to 600 bar*, Geochim. Cosmochim. Acta 69 (13), 3309–3320, 2005.

Steefel, C.I, A.C. Lasaga, *A coupled model for transport of multiple chemical species and kinetic precipitation/dissolution reactions with applications to reactive flow in single phase hydrothermal system*, Am. J. Sci.; 294:529–92, 1994.

Tamini, A., Rinker, B., Sandall, O.C., Diffusion Coefficients for Hydrogen Sulfide, Carbon Dioxide, and Nitrous Oxide in water over the Temperature Range 293-368 K, J.Chem.Eng.Data, 39, 330-332, 1994

Verma, A. and K. Pruess, *Thermohydrologic Conditions and Silica Redistribution Near High-Level Nuclear Wastes Emplaced in Saturated Geological Formations*, J. of Geophys. Res.,Vol. 93, No. B2, pp. 1159-1173, 1988.

Wang L.S., Lang Z.X., Guo T.M., *Measurement and correlation of the diffusion coefficients of carbon dioxide in liquid hydrocarbon under elevated pressures*, Fluid Phase Equilibria, 117, 364-372, 1996

Wolery, T.J., *EQ3/6: Software package for geochemical modeling of aqueous systems: package overview and installationguide (version 7.2)*, Lawrence Livermore National Laboratory Report UCRL-MA-10662 PT I, Livermore, California, 1992.

Xu, T., K. Pruess, *Modeling multiphase non-isothermal fluid flow and reactive geochemical transport in variably saturated fractured rocks: 1 Methodology*, Am. J. Sci. 301, 16–33, 2001.

Xu, T., E.L. Sonnenthal, N. Spycher, K. Pruess, *TOURGHREACT: a simulation program for non-isothermal multiphase reactive geochemical transport in variably saturated geologic media*, Comput. Geosci. 32, 145–165, 2006.